# Molecular Beam Epitaxy of Ga(In)AsN/GaAs Quantum Wells towards 1.3μm and 1.55μm

S.Z.Wang, S.F.Yoon, T.K.Ng, W.K.Loke, and W.J.Fan

*Abstract* — In this article, we report an attempt of extending the InGaAsN materials towards 1.3μm and 1.55μm wavelength. All these InGaAsN samples are grown in a plasma-assisted solid-source molecular-beam epitaxy (SS-MBE) system. Our experiments revealed that the nitrides could be grown with both direct nitrogen beam and dispersive nitrogen. The nitrogen incorporation rate could be reduced by the presence of indium flux. The interaction between nitrogen and indium might lead to 3D growth mode and growth dynamics. It is proved that the increasing growth rate reduces the nitrogen incorporation efficiency. The data for nitrogen sticking coefficient are somewhat contradictive. The growth with dispersive nitrogen source causes the improvement of material quality. Fixed indium flux is a better way for the wavelength control. Also, we report some growth optimization work for better PL property and the annealing effect on the samples. Literature is sometimes reviewed for comparison.

*Keywords* — In(Ga)AsN/GaAs, Quantum wells, Molecular beam epitaxy, 1.3μm, 1.55μm.

## I. INTRODUCTION

Semiconductor lasers emitting at 1.3μm and 1.55μm are of fundamental importance in optical communication systems. The presently used InGaAs/InGaAsP and InGaAsP/InP 1.3μm and 1.55μm lasers have a poor characteristic temperature($T_0$), with a typical value of ~60K[1], and subsequently, cooling systems are needed. These devices have been long expected to operate stably over a wide temperature range, without thermoelectric cooling, which requires a high characteristic temperature $T_0$. A novel material, InGaAsN/GaAs, has been proposed to solve this problem[2]. The high conduction-band discontinuity of possibly more than 300meV at the interface of the III-(V,N)/III-V heterostructure has the potential of creating semiconductor lasers with high characteristic temperature $T_0$ exceeding 150K[2]. The InGaAsN/GaAs laser diodes operating at 1.3_m and 1.55μm wavelength have been demonstrated, respectively[3][4]. Indeed recently, a $T_0$ value of 148K was demonstrated in GaInAsN/GaAs quantum well lasers emitting at 1.3_m[5]. Electrically pumped vertical cavity surface emitting lasers (VCSELs) have also been reported[6].

Recent attempts have been focused on obtaining GaAs-based nitrides of sufficiently high quality for the fabrication of laser diodes. However, the InGaAsN quality deteriorates dramatically with increasing nitrogen composition due to a large miscibility gap and phase separation, even though the amount of average strain in the epilayer decreases, as compared with the relevant InGaAs epilayer with the same indium composition. In an attempt of increasing the material quality, a number of epitaxial techniques have been reportedly used for growing GaAs-based nitrides. These include metalorganic chemical vapor deposition (MOCVD)[7], molecular beam epitaxy (MBE)[8] and metalorganic molecular beam epitaxy (MOMBE)[9]. It is often known that most nitrides are relatively stable at the growth temperatures used in MOCVD due to the strong N-X bonds, hence making it difficult to incorporate nitrogen atoms into GaAs. Using the plasma-assisted MBE technique, a large nitrogen concentration in excess of 10%[10] has been successfully incorporated into the GaAsN materials. So far, the plasma-assisted MBE technique seems the best successful one for the growth of InGaAsN materials.

In this article, we report an attempt of extending the InGaAsN materials towards 1.3μm and 1.55μm wavelength. All these InGaAsN samples are grown in a plasma-assisted solid-source molecular-beam epitaxy (SS-MBE) system. Our experiments revealed that the interaction between nitrogen and indium might determine the growth mode and growth dynamics. We also reported the nitrogen incorporation behavior during MBE growth somewhat different from what the literature have reported, the modified growth mode tried for higher quality nitrides, the wavelength control of epilayers, the growth optimization for better photoluminescence (PL) property, and the annealing effect on the samples. Also, literature is reviewed for comparison.

S.Z. Wang is with the Innovation in Manufacturing Systems and Technology (IMST) Singapore-Massachusetts Institute of Technology(MIT) Alliance, N2-B2C-15 Nanyang Technological University, 50 Nanyang Avenue, Singapore 639798, Email address: szwang@ntu.edu.sg;

S.F. Yoon is with the Innovation in Manufacturing Systems and Technology (IMST) Singapore-Massachusetts Institute of Technology(MIT) Alliance, N2-B2C-15 Nanyang Technological University, 50 Nanyang Avenue, Singapore 639798, Email address: esfyoon@ntu.edu.sg

T.K. Ng is with the School of Electrical and Electronic Engineering, Microelectronics Center, Nanyang Technological University, Nanyang Avenue, Singapore 639798,

W.K. Loke is with the School of Electrical and Electronic Engineering, Microelectronics Center, Nanyang Technological University, Nanyang Avenue, Singapore 639798,

W.J. Fan is with the School of Electrical and Electronic Engineering, Microelectronics Center, Nanyang Technological University, Nanyang Avenue, Singapore 639798,

## II. EXPERIMENTAL DETAILS

The GaAsN and InGaAsN samples were grown in a SS-MBE system, equipped with five standard effusion cells for indium, gallium, aluminum, beryllium and silicon, three cracker cells for arsenic, phosphorous and hydrogen, and one plasma source for nitrogen, respectively. The purity of all the source charges is six nines. All samples were grown on (001)-oriented semi-insulating GaAs substrates prepared using standard preparation procedures. Prior to growth, the surface oxide desorption was carried out under $As_4$ flux at a beam equivalent pressure (BEP) of $6.2X10^{-6}$ torr. A (2X4) surface reconstruction was maintained during the entire growth process. The beam equivalent pressures used for Ga and As were $4.5X10^{-7}$ torr and $6.2X10^{-6}$ torr, respectively. The V/III ratio was fixed at about 14 for the growth of all samples. The Ga and As fluxes were adjusted by controlling the temperature of the effusion cells. The above BEPs result in a growth rate of ~1.0 _m/h verified by time resolved RHEED measurements. The nitrogen plasma source works at nitrogen background pressure of $3.6X10^{-6}$ torr in the presence of $As_4$ ($6.2X10^{-6}$ torr) and is activated by radio frequency (R.F.) power greater than 60 W to maintain the plasma in high brightness mode.

An undoped GaAs buffer layer was first grown onto the GaAs substrate at $590^{o}$C. The substrate temperature was then reduced to the desired value of $460^{o}$C for growth of the following individual GaAsN/GaAs, InGaAs/GaAs, InGaAsN/GaAs structures and their combined structures. A GaAs cap layer was then grown on the top of nitrides. XRD measurements were carried out on the samples, and PL experiments were carried out using an optical system designed specially for compound semiconductors over a temperature range from 4.2K to 300K. Excitation was at near normal incidence using a 514.5nm beam from an Ar ion laser. The PL signals were collected with a dual grating spectrometer in the reflection direction and then detected using a liquid nitrogen cooled germanium (Ge) detector in association with a standard lock-in technique.

## III. RESULTS AND DISCUSSION

*A. Nitrogen source characteristics*

The R.F.-activated nitrogen plasma source is, to our experience, one of the most complicated MBE sources. The working character of the nitrogen plasma source is fundamentally different from the conventional effusion cell, in the way the raw material is activated (by a R.F. power supply other than by an electrical resistance) and in the natural state the raw material is kept (gas state other than solid state). An extensively known fact is that the plasma source only works over a certain pressure range of the gas material. The gas material cannot be discharged beyond this pressure range. Only at a certain pressure value amongst this pressure range, can the gas material be activated most effectively. What is more, the concentration of the active species shows a saturation character as the activated power is increased, due to the decrease of the coupling factor of the R.F. power.

Therefore, it is necessary to familiarize us with the special plasma source before the growth of InGaAsN.
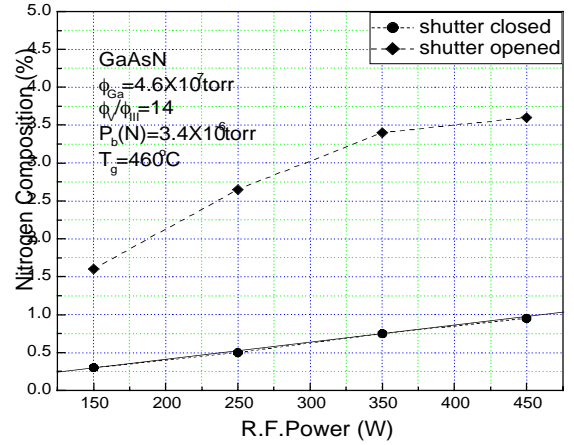


Fig.1: Experimental and fitting results of nitrogen composition in GaAsN layer *vs.* R.F. power of the nitrogen plasma source, under conditions indicated in the figure. [♦ : nitrogen composition in GaAsN grown with direct nitrogen beam, • : nitrogen composition in GaAsN epilayers grown with dispersive nitrogen source]

The optimal background nitrogen pressure for the effective operation of the plasma source is ~$3.4X10^{-6}$ torr, for our MBE configuration. All nitride growths afterwards are conducted under this optimal pressure. Fig.1 shows the relationship between the nitrogen composition of GaAsN epilayers and the R.F. power applied to the plasma source. As we have described in a separate paper[11], the nitrides can be grown with both nitrogen beam from the plasma source and dispersive nitrogen from the background. The diamond marks indicate the nitrogen composition of GaAsN grown with nitrogen beam from the plasma source, while the dot marks denote the corresponding nitrogen composition of GaAsN epilayers grown with dispersive nitrogen source. It is noticeable that whatever the growth is accomplished with nitrogen beam or dispersive nitrogen source, the nitrogen composition of GaAsN epilayer increases monotonously as the activation power increases. Our experiments revealed that the nitrogen flux of the direct nitrogen beam is ~$2.0X10^{-7}$ torr. Therefore, the solid diamond symbols represent the combined nitrogen composition data caused by the direct nitrogen beam and active nitrogen in the chamber background. The solid line fitted through the solid dots is obtained by assuming the number of the active nitrogen species in background is a linear function of the activation power. The excellent agreement between the fitting result and the experimental data imply that the linear relationship assumption between the active nitrogen concentration and the activation power is reasonable[11]. Nevertheless, the nitrogen composition of GaAsN epilayer grown with activated nitrogen beam shows a superlinearity over the increased R.F. power, suggesting a saturation

behavior of nitrogen incorporation. Because the nitrogen composition contributed by the dispersive nitrogen does not show any deviation from linearity, the saturation behavior of nitrogen can only ascribed to the saturation of the activated nitrogen flux spurting out from the plasma source, due to the decrease of coupling factor of R.F. power. This explanation is reasonable, because the nitrogen within plasma source has a pressure as low as $10^{-2}torr \sim 10^{-4}torr$, and there is a limit to which the R.F. power can be coupled to nitrogen gas. However, our experiments have proved that nitride samples grown with dispersive nitrogen are of higher crystalline, interface and optical quality than those grown with direct nitrogen beam[12].

## B. Nitrogen-indium interaction
### B.1 Nitrogen incorporation rate effected by nitrogen-indium interaction

The indium composition of InGaAs epilayer could be well controlled by adjusting the indium flux, as is much easier than the control of nitrogen composition in GaAsN. The indium composition of InGaAs epilayer increases linearly with the indium flux. Harmand and Tournie et al[13][14] reported that the nitrogen incorporation rate was independent on the presence of indium flux, where the R.F. plasma cell was basically the same as our nitrogen source. However, our results tend to show that the nitrogen incorporation efficiency is lowered by the presence of indium flux. Fig.2 shows the PL spectra at 4.2K of two quantum well samples with different indium composition 25% and 36% respectively for MN042 and MN041 samples. An 8nm wide InGaAsN quantum well is grown onto a 300nm thick GaAs buffer layer immediately after the buffer growth, then a 100nm thick GaAs is grown on the top of InGaAsN well, contemporarily serving as barrier/isolation layer of/between the InGaAsN quantum well and a followed 8nm wide InGaAs quantum well. Finally, the InGaAs quantum well is covered with a 20nm thick GaAs cap layer. The indium flux for InGaAs quantum well is controlled same as that for InGaAsN quantum well, so that the InGaAs quantum well serves as a reference structure in X-ray diffraction (XRD) and PL measurements. The 986nm PL peak from the
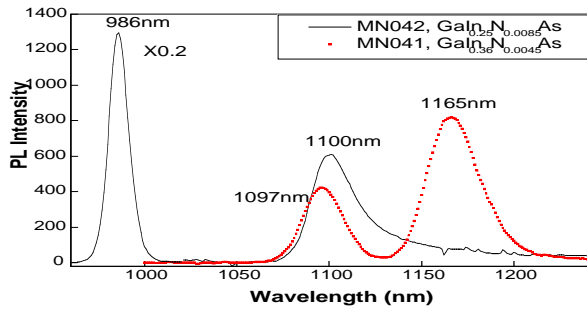


Fig.2: The PL spectra from two InGaAs/GaAsInGaAsN/GaAs double quantum well samples with different nitrogen and indium composition.

InGaAs well serves as a reference peak for the 1100nm peak from the $In_{0.25}GaAsN_{0.0085}$ well, similarly, the 1097nm PL peak from the InGaAs well serves as a reference peak for the 1165nm peak from the $In_{0.36}GaAsN_{0.0045}$ well. The growth condition for these two samples are retained same except for the indium flux for different indium composition. However, the nitrogen composition of MN042 and MN041 samples is different as 0.85% and 0.45% respectively. That implies that the nitrogen incorporation efficiency could be apparently reduced by the presence of indium flux. This effect is testified by growing GaAsN epilayer under the same growth condition, in which the nitrogen composition is 1.0%. Fig.3 shows the nitrogen composition as a function of the indium composition. The squares denote the nitrogen composition data of MN041 and MN042 InGaAsN samples, as well as the nitrogen composition of the relevant GaAsN sample (i.e., let the indium cell closed). The dots show the nitrogen values that are nomoalized to the relevant GaAsN case at the equivalent growth rate. The solid and dashed lines are for eye-guidance. It is clear that the nitrogen composition of InGaAsN epilayer decreases as the indium composition increases even though the
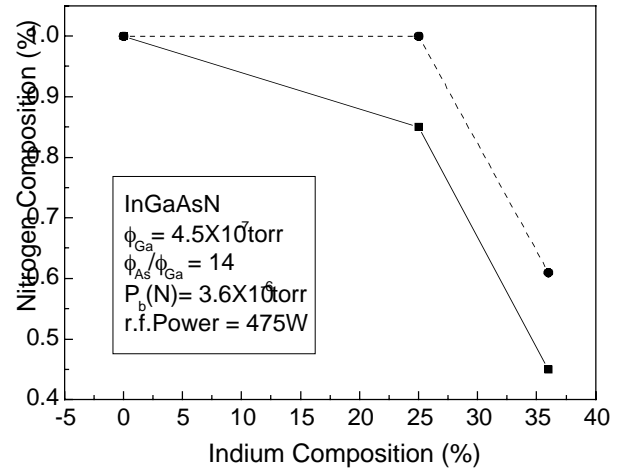


Fig.3: The relationship between the nitrogen composition and indium composition in InGaAsN epilayers, under the growth conditions indicated in the figure.

growth rate is normalized to the relevant GaAsN case. The experimental results are somewhat different from Harmand and Tournie's results obtained from SS-MBE system [13][14], but agree with the GS-MBE results[15]. We will show the evidence, later in this article, to that the nitrogen composition in GaAsN epilayer could be decreased by the increasing growth rate. However, it is noticeable from Fig.3 that the nitrogen composition is not decreased linearly by the increasing growth rate. If the nitrogen composition is decreased linearly by the increasing growth rate, then the normalized nitrogen composition of all nitride samples should be the same.

*B.2 Growth mode determined by nitrogen-indium interaction*

Our experiments reveal that even though the RHEED pattern shows a clearly streaky (2X4) reconstruction during the growth of the 6.5nm wide $In_{0.30}Ga_{0.70}As$ quantum well layer, the RHEED pattern for the 6.5nm wide $In_{0.30}Ga_{0.70}As_{1-x}N_x$ quantum well layer usually shows a partially spotty structure with no reconstruction. That implies that the interaction between nitrogen atom and indium atom on the growth surface may facilitate the formation of the three-dimension (3D) growth mode and therefore degrade the material quality, even though the nitrogen incorporation generally decreases the average strain of the InGaAsN epilayer. Our RHEED pattern is in accordance to the Pan's observation [16], where only the RHEED phenomena were stated without any explanation. Our conjecture, that indium and nitrogen atoms tend to gather on the growth surface to form dot-like structures, can be confirmed by transparent electron micrograph (TEM) investigation, where clearly shown the gathering behavior of indium and nitrogen and the formation of indium-rich and nitrogen-rich dot-like structures [17]. Consequently, there should be many island-like structures presented on the growth surface. Fig.4 is a light microscopic picture of the InGaAsN growth surface. Actually, there are island-like structures on the growth surface. The dimension of the islands is about 100nmx200nm, with the long axis self-organized along with a certain orientation. Kitatani have reported the strong emission from the dot-like structures amongst InGaAsN quantum well [18]. According to Pan's RHEED observation, enhanced surface migration might benefit the formation of the dot-like structures, since the increase in growth temperature directly lead to the transformation of RHEED pattern from streaky to spotty mode. The formation mechanism of the dot-like structures may finally determine the upper edge of the growth temperature window of the InGaAsN materials.



Fig.4: A light microscopic picture of the InGaAsN growth surface.

*C. Nitrogen incorporation behavior*

*C.1 Nitrogen incorporation efficiency affected by growth rate*

In section B.1, we have revealed that the presence of indium may decrease the nitrogen incorporation efficiency. In order to investigate whether the reduction of the nitrogen incorporation

efficiency is caused by the increased growth rate in the presence of Indium, we checked the growth rate effect on the nitrogen incorporation efficiency in GaAsN. Fig.5 shows the relationship between the nitrogen composition of GaAsN epilayer and its growth rate. It is clear that the nitrogen composition of GaAsN epilayer reduces as the growth rate increases. For example, the nitrogen composition in GaAsN sample is 2.82% when the growth rate is controlled at 0.5μm/hr, while the growth rate is increased up to 1.0μm/hr, the nitrogen composition in GaAsN sample reduced down to 2.03%. That implies that the nitrogen in principle behaves like a dopant in the GaAsN growth. Therefore, the reduction of the nitrogen composition in the growth of InGaAsN could be suspect due to the growth rate increase caused by the presence of indium flux. The dashed line indicates a theoretical result supposing the nitrogen composition of GaAsN layer decreases linearly with the growth rate increase. It is noticeable that there is a deviation of the experimental results from the linearity assumption, and the reason for the deviation of experimental data from the linearity is under investigation. However, our result is somewhat different from Egorov and Spruytte's report, where they showed a linear relationship between the nitrogen composition in GaAsN and the growth rate [19][20].
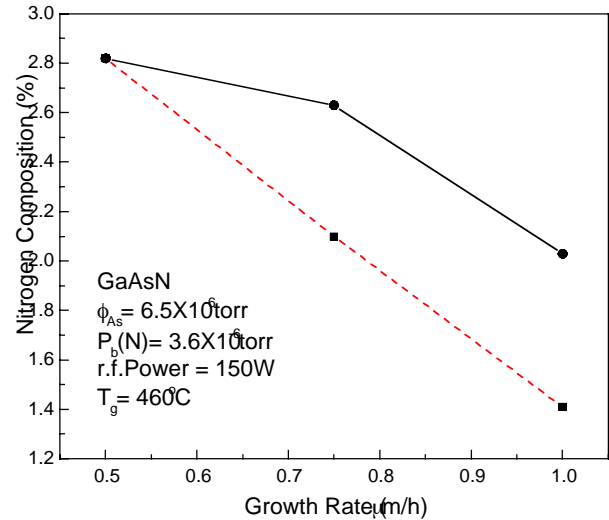


Fig.5: The relationship between the nitrogen composition and growth rate of GaAsN epilayer, under the growth conditions indicated in the figure.

*C.2 Nitrogen sticking coefficient*

There are some contradictive results on nitrogen sticking coefficient. Egorov showed a complicated relationship between nitrogen sticking coefficient and arsenic to nitrogen ratio as,

$$K_{STIC} = A \log(F_{As}/F_N+1) \quad (1)$$

where, $K_{STIC}$ is nitrogen sticking coefficient, A is a proportion constant, $F_{As}$ and $F_N$ are arsenic and nitrogen flux,

respectively[19]. However, Kitatani reported that the sticking coefficient of atomic nitrogen is effectively unity[21]. In fact, it is the complication of nitrogen incorporation behavior that warrants further investigation.

### D. Wavelength control

It is known from the aforementioned statement that the indium flux could effect the nitrogen composition of InGaAsN, therefore, it is a better way to fix indium flux than to fix the nitrogen source condition in the growth of InGaAsN. Because firstly the nitrogen behaves like a dopant in the growth of InGaAsN, the indium composition is therefore not effected by the nitrogen incorporation. Even though the nitrogen could effect the indium composition of InGaAsN epilayer, however, the nitrogen composition is only lower than 2%, the effect could be omitted. Fig.6 is the growth results obtained by fixing indium composition at ~34% and adjusting nitrogen source condition. The structures of MN043, MN044 and MN045 samples are same as that of MN041 and MN042 samples. The growth reproducibility is testified with the reference PL
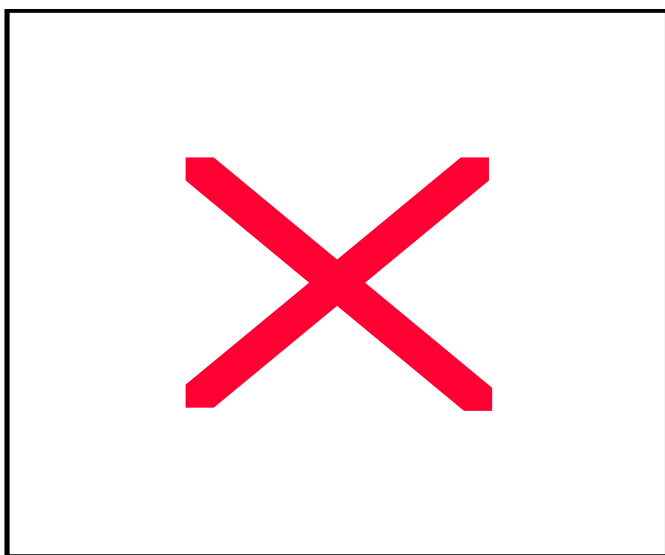


Fig.6: The PL spectra from three InGaAs/GaAsInGaAsN/GaAs double quantum well samples with different nitrogen composition and nominally with the same indium composition.

peaks at 1054nm, 1081nm and 1086nm respectively from relevant InGaAs reference quantum wells, which are specially grown as reference structures for the InGaAsN quantum wells. The right-hand three PL peaks at 1333nm, 1464nm and 1500nm respectively from $In_{0.32}GaAsN_{0.015}$, $In_{0.34}GaAsN_{0.02}$ and $In_{0.35}GaAsN_{0.021}$ quantum wells are obtained by adjusting the nitrogen plasma source. The results indicate that the growth is more controllable by keeping the indium composition fixed firstly and leaving the nitrogen adjustable, than vise versa.

### E. Bombardment effect

Fig.7 shows two XRD rocking curves of the GaAsN layers at (004) diffraction direction. The solid curve is data from the sample grown with dispersive nitrogen source, and the dashed curve is data from the sample grown using direct nitrogen beam. With reference to the GaAs substrate peak, the GaAsN peak is easily identifiable, and the nitrogen composition deduced from the simulation result is ~1.3%. This is in good agreement with the nitrogen composition result of ~1.3% deduced from secondary ion mass spectroscopy (SIMS) measurement. Consistent with the RHEED pattern observations, the strong XRD peak further testifies to the high quality of the GaAsN epilayer. Strong fringes are also observed in both XRD spectra, indicating the presence of smooth and abrupt GaAsN/GaAs interface. The XRD result of our sample grown with dispersive nitrogen source has smaller full-width at half maximum (FWHM) value compared to that reported by Harmand[13], where the reported nitrogen composition is ~1.1% to ~1.2%. In addition to the fact that the XRD peak of the sample grown with dispersive nitrogen source is stronger than that of the sample grown with direct nitrogen beam, the FWHM of the XRD peak of the sample grown with dispersive nitrogen source is also narrower than that of the sample grown using direct nitrogen beam (195 arcsec vs. 251 arcsec). This clearly indicates higher crystalline quality in the sample grown with dispersive nitrogen source compared to the sample grown using direct nitrogen beam. Furthermore, the sample grown with dispersive nitrogen source has more fringes in the XRD spectrum, indicating the presence of a smoother and more abrupt interface between the GaAsN layer and GaAs layer.
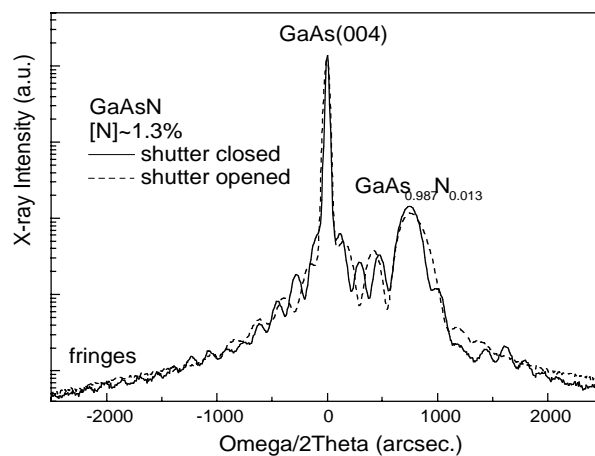


Fig.7: XRD rocking curve of the as-grown GaAsN epilayer in the (004) diffraction direction. The solid curve is data from the sample grown with dispersive nitrogen source, and the dashed curve is data from the sample grown using direct nitrogen beam.

In a R.F.-activated direct nitrogen beam process, the nitrogen species include N atoms, $N^+$ and $N_2^+$ ions, and metastable $N^*$ atoms and $N_2^*$ molecules in the excited states[22][23]. The excited molecular species such as $N_2^+$ and $N_2^*$ are the effective reactive species, which are readily incorporated into the material to form clusters due to difficulty to break the extremely strong N-N chemical bonds at the low substrate temperature in MBE growth. Thus, both the crystalline and interface quality of the material can be degraded by the presence of $N_2^+$ and $N_2^*$ reactive species. This is the reason why the sample grown with direct nitrogen beam has a broader XRD peak and fewer fringes in the spectrum. In the case of dispersive nitrogen source, the $N_2^+$ ions are neutralized, and the $N_2^*$ molecules are relaxed to the ground state to form $N_2$ molecules. These $N_2$ molecules then become part of the $N_2$ background, which does not participate in the growth process. The advantages of using the dispersive nitrogen source in MBE growth of GaAsN are further testified with the following experimental evidence.

Fig.8 shows two PL spectra of the  GaAsN epilayers at 4K. The solid curve is the data from the sample grown with dispersive nitrogen source, and the dashed curve is the data from the sample grown using direct nitrogen beam. The PL peaks of both spectra located at ~1034nm (~1.2eV), are consistent with the XRD results. It is noted that the PL peak of the sample grown with dispersive nitrogen source is much stronger than that of the sample grown with direct nitrogen beam. Furthermore, the FWHM of the PL peak of the sample grown with dispersive nitrogen source is as narrow as 42.4meV. This is significantly smaller than that of the sample grown with direct nitrogen beam of 99.2meV, indicating the higher crystalline quality in the sample grown with dispersive nitrogen source. Moreover, the sample grown with direct nitrogen beam has a prominent low-energy tail in the PL spectrum, the reason for which is unclear at this moment. Li [24] has attributed the poor optical properties of their as-grown samples to several possible reasons such as implantation damage, presence of group-V vacancies and impurities. In the case of our samples, the growth conditions are essentially the same, except for the manner in which the nitrogen is introduced (dispersive *vs*. direct nitrogen beam). Hence, this suggests that the concentration of group-V vacancies and impurities are essentially the same. However, since the PL properties of the samples grown using dispersive nitrogen source and direct nitrogen beam are quite different, therefore the group-V vacancies and impurities could not be the main mechanism responsible for the poor optical property of the material. Therefore, it is highly probable in our case that the use of the dispersive nitrogen mode during growth has significantly reduced the effects of implantation damage due to the energetic nitrogen ions, hence improving the optical quality of the sample. Although the low-energy tail in the PL spectrum has been suppressed by the use of the dispersive nitrogen mode, the PL peak of GaAsN is not as narrow as expected. The reasons for the broadening and presence of the low energy tail in the PL spectrum, and ways to improve the optical property of the material warrant further investigation on the growth mechanism. Since the PL measurement was performed at 4K, it is probable that the PL emission comes from the radiative recombination of excitons in the unintentionally doped GaAsN material, and the low energy emission arises from the defect related mid-gap energy levels.
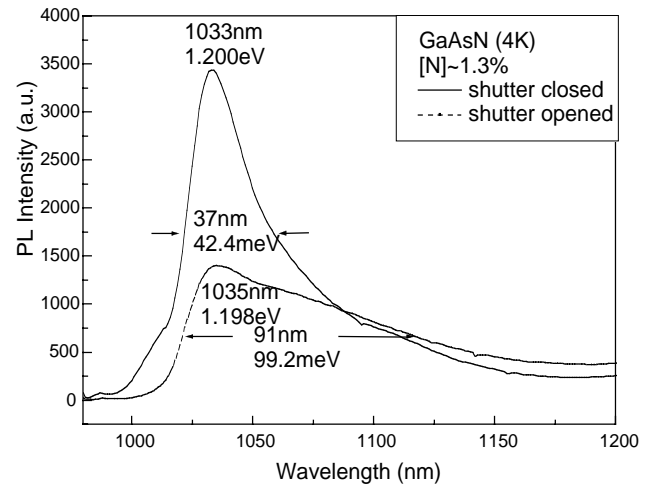


Fig.8: Low temperature (4K) PL spectra of as-grown GaAsN epilayers. The solid curve is data from the sample grown with dispersive nitrogen source, and the dashed curve is data from the sample grown using direct nitrogen beam.

Fig.9 compares two typical light microscopy pictures of the GaAsN surface of samples grown using (a) the dispersive nitrogen growth mode, and (b) the direct nitrogen beam growth mode. This preliminary comparison shows that the GaAsN sample grown using dispersive nitrogen have fewer defects on the surface than that grown with direct nitrogen beam from the plasma activated nitrogen source. In fact from our experience, it is rather difficult to find a view spot with several defects on the surface of the GaAsN sample grown using dispersive nitrogen. On the contrary, there are many defects on the surface of the GaAsN sample grown using direct nitrogen beam. It is unclear whether the reduced number of surface defects on the sample grown using dispersive nitrogen was due to the lower bombardment effect of energetic nitrogen ions, an aspect which requires more detailed investigation. Nevertheless, this observation is in reasonable agreement with the PL measurement results.

When the growth temperature is decreased lower than $440^{\circ}$C, the efficiency of rediative recombination of InGaAsN, even InGaAs, could be dramatically decreased, giving evidence to the degradation of critical quality, as is common for any MBE grown materials. The temperature of $440^{\circ}$C therefore acts as the low edge of the temperature window for the InGaAsN growth. On the other hand, when the growth temperature is ramped higher than $500^{\circ}$C, the decrease in the nitrogen incorporation could be very severely, see Fig.10, leading to problems to research the target wavelength. Another side effect of the increased growth temperature is that it may lead to degradation of the surface morphology, and consequently the crystal quality, which is evidenced
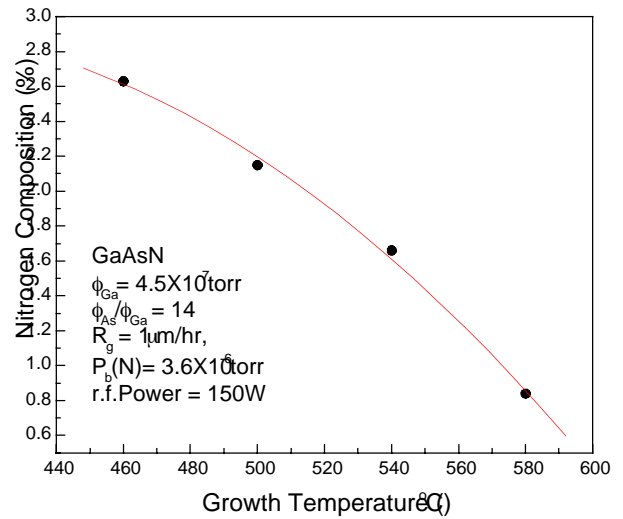


Fig.10: The relationship between the nitrogen composition and growth temperature of GaAsN epilayer, under the growth conditions indicated in the figure. The dots show the experimental data and the curve is the guideline for eye.

by the catastrophic decrease in the PL intensity of InGaAsN samples. The temperature of $500^{\circ}$C is therefore regarded as the upper edge of the temperature window for the InGaAsN growth. For our case, the growth temperature window for InGaAsN is concluded be $440^{\circ}$C-$500^{\circ}$C or narrower, which is coincident with the literature [19][25]. Thus, the temperature control of the substrate is something very important for the growth of desired InGaAsN epilayer.

*(a)*

*(b)*

Fig.9: Optical microscopy pictures (X1000) of the surface of GaAsN epilayers grown using (a) dispersive nitrogen growth mode, and (b) direct nitrogen beam growth mode.

*F. Growth temperature window*

There are two factors finally deciding the temperature window for the growth of InGaAsN, and the temperature window could put effect on the material quality seriously.

*G. Growth optimization*

For the device fabrication, the PL linewidth is a more important parameter than the PL intensity. Fig.11(a) shows the relationship between the PL intensity and the indium/nitrogen composition of InGaAsN samples, and Fig.11(b) gives the relationship between the PL linewidth and the indium/nitrogen composition of InGaAsN samples. It is noticeable that the maximum PL intensity and the minimum PL linewidth both

appear at the right-bottom corner, which acquires low indium and low nitrogen composition of InGaAsN samples. However, moderate quantity indium as well as nitrogen is required so as to reach the desired wavelength with InGaAsN. As have known, there is a big misibility gap in between GaAs and GaN binaries. A small nitrogen composition as low as 5% could degrade the (In)GaAsN quality greatly, leading to catastrophic decrease in PL intensity. This sort of degradation is not limited by the conventional critical thickness. While the degradation due to indium is guided by the critical thickness. Therefore, for a quantum well with certain wellwidth, it is better to add more indium and less nitrogen so as to reach the desired wavelength, so long as the quality of InGaAs material is acceptable. A very important experimental phenomenon that I would like to point out here is that, even though the RHEED patterns during the growths of GaAsN and InGaAs with same nitrogen composition and indium composition as the relevant InGaAsN are keep streaky, the RHEED pattern for the InGaAsN is tendentious to be spotty. That implies the interaction between nitrogen atom and indium atom on the growth surface may have the tendency to form a three-dimension (3D) growth mode and degrade the material quality.

**InGaAsN QW linewidth (eV)**
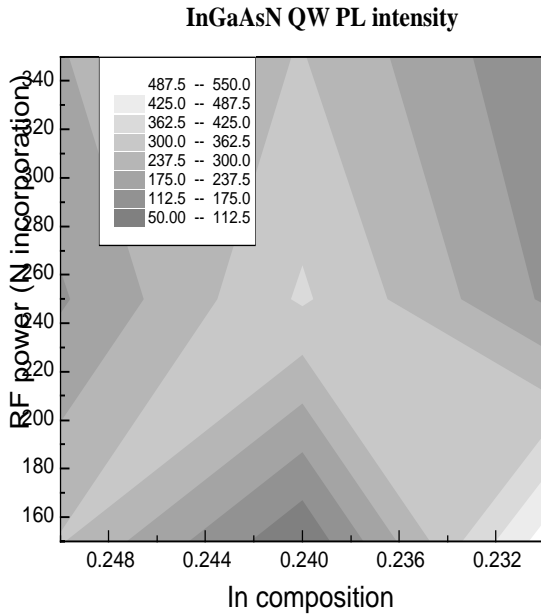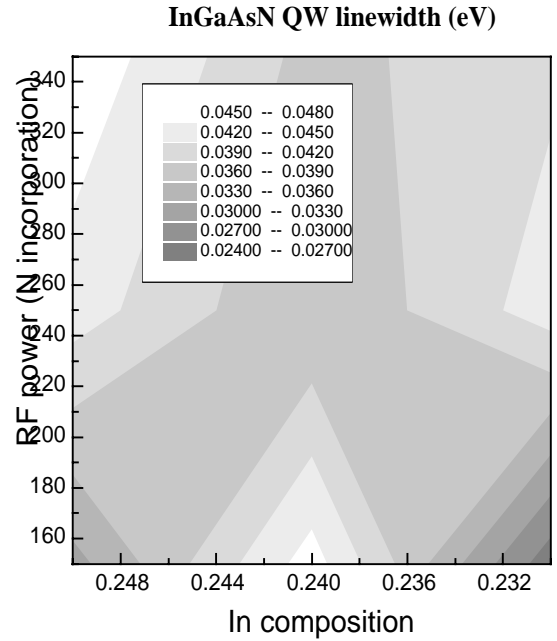


(b)

Fig.11: (a) The relationship in between the PL intensity and the indium/nitrogen composition of InGaAsN samples. (b) The relationship in between the PL linewidth and the indium/nitrogen composition of InGaAsN samples.

*H. Annealing Effect[26]*

The GaInAs quantum well (QW) of Sample A have lower In composition (22%) as compared to that of Sample B (30%), and therefore the GaInAs QW of Sample A emits at a lower wavelength (see Fig.12(a)) as compared to that of Sample B (see Fig.12(b)). Due to the increase in growth rate as a results of more incoming In flux during the growth process of Sample B, the amount of nitrogen incorporated in GaInNAs would be reduced and hence this would results in smaller difference between the peak positions of the as-grown GaInAs and GaInNAs QWs for Sample B ($8\lambda_{B,as-grown}$) as compared to that of Sample A ($8\lambda_{A,as-grown}$). This is evident in the experimental results where the value of $8\lambda_{B,as-grown}$ (80nm) is smaller than that of $8\lambda_{A,as-grown}$ (143nm).

The continuous line of Fig.12(a) shows the as-grown photoluminescence (PL) spectra of Sample A measured at 4.5K. The as-grown GaInAs quantum well (QW) shows a high intensity of 3500 a.u. at 950.5nm with a FWHM of 7.8meV. However the as-grown GaInNAs QW (Fig.12(a)) exhibits poor PL characteristics indicating highly defective material. Annealing at 840°C for 10min shows tremendous increase in the GaInNAs emission intensity by 30 times to 6700 a.u. and

**InGaAsN QW PL intensity**



(a)

reduction in full-width-at-half-maximum (FHWM) from 63.1meV to 16.3meV, which is comparable to the results reported in the existing literature [27][28]. This indicates a high crystal quality GaInNAs quantum well after post-growth thermal annealing (PTA) process. As for GaInAs, the growth temperature of $480^{o}C$ (see Table I) is lower than the optimised temperature of $500^{o}C$ reported in existing literature and hence the degraded quality could be improved if proper annealing was carried out. This is evident in Fig.12(a) where the FWHM of GaInAs after annealing (7.2meV) is comparable to the value before annealing (7.8meV). This together with the improvement of GaInNAs QW after annealing justifies the suitability of the high annealing temperature $(840^{o}C)$ and long period of time (10min) used for this study.

PTA has resulted in a significant reduction in the FWHM of GaInNAs QW from 63.1meV to 16.3meV as mentioned in the above. The origin of the improvement of the GaInAs and GaInNAs QW crystal quality was suggested to be annealing temperature dependent by Pan [29]. Firstly, removal of nitrogen-ion-damage at interfaces through defect-assisted N and As diffusion effect has been suggested to occur at low annealing temperature (less than $800^{o}C$) during the initial stage of annealing. Secondly, high temperature annealing process further removes the defects caused by insufficient migration of Ga and In during low temperature growth [29][30]. This study indeed found the removal of defects due to the enhancement of Ga and In migration, which is reflected in the increase in the intensity of the GaInAs peak in Fig.12(a). Since the annealing temperature of $840^{o}C$ used for this study is well above $800^{o}C$, the PTA process would results in both elimination of nitrogen-ion-induced damage as well as enhancement of Ga and In migration. Therefore, better GaInNAs crystal quality of Sample A (see Fig.12(a)) in terms of higher PL intensity and smaller FWHM of the annealed QW is observed.

In order to understand the mechanism of peak wavelength shifting after PTA, the GaInAs QWs are first examined. The interface diffusion of the host atoms such as Ga and In is clearly shown in Fig.12(a) where the PL peak position of GaInAs (Sample A) has shifted from 950.5nm to a lower wavelength of 941 nm after PTA (a change in wavelength of $8\lambda_{A,GaInAs}=10nm$). The highly defective as-grown GaInAs material shows a much larger wavelength shift of $8\lambda_{A,GaInNAs}=70nm$ (from 1093nm to 1021nm, see Fig.12(a)) after PTA due to In-Ga interface interdiffusion and nitrogen-ion-damage-defect-assisted diffusion. As for Sample B, the PL peak position of GaInAs has shifted from 1021nm to a lower wavelength of 962nm after PTA and that of GaInNAs has shifted from 1101.5nm to 1014.5nm. The change in wavelength of the GaInAs QW of Sample B ($8\lambda_{B,GaInAs}=60nm$) is much larger than that of Sample A ($8\lambda_{A,GaInAs}=10nm$).

| Details | Sample A (73) | Sample B (74) |
|---|---|---|
| GaAs Cap | 80nm | 80nm |
| GaInAs | 6nm | 6nm |
| GaAs Isolation | 100nm | 100nm |
| GaInNAs | 6.5nm | 6.5nm |
| GaAs Buffer | 300nm | 300nm |
| Growth Temp | $480\ ^{o}C$ | $480\ ^{o}C$ |
| In BEP | $2.1\times10^{-7}$ | $2.8\times10^{-7}$ |

As the annealing temperature used for both Sample A and Sample B are the same and both having identical growth conditions with the exception of In flux, the mechanism of the large wavelength shift in this study would not be annealing temperature dependent but In composition dependent. It is suggested in this paper that the larger value of In composition, and therefore $8\lambda_{B,GaInNAs}$, at high temperature could be caused by both the residual-strain induced interdiffusion [31] and the defect-induced interdiffusion as a results of In incorporation. As Sample B has higher In composition, more severe residual-strain-induced interdiffusion of Ga and In at the GaInAs/GaAs interface may occur. On the other hand, Sample A has lower In composition and therefore less severe strain-induced interdiffusion could occur. Also, the argument of defect-assisted interdiffusion of GaInAs during annealing is supported by the lower crystal quality of the as-grown GaInAs QW of Sample B as seen in the PL FWHM. The FWHM of 14.5 meV is larger than that of the as-grown GaInAs QW of Sample A (7.8meV), and hence correlates well with the reflection high energy electron diffraction (RHEED) observation during growth. It shows that the time required for Sample B (higher In composition) to transform from streaky (2x4) surface reconstruction to short-line (2x1) surface reconstruction during the initial stage of GaInAs QW growth was much shorter than that of Sample A. The RHEED observation shows that three-dimensional (3D) growth as a results of surface strain happened earlier in Sample B than in Sample A. The 3D growth results in more defects in Sample B, and therefore lower crystal quality of Sample B as compared to Sample A.

Following the above argument of residual-strain-induced interface interdiffusion and the defect-assisted diffusion in GaInAs QW, it would be expected that the GaInNAs QW of

Sample B would show a larger shift as compared to that of Sample A. This is indeed observed in Fig.12(a) as the change in the wavelengths of the GaInNAs QWs of Sample B before and after PTA ($8\lambda_{B,GaInNAs}$=87nm) is larger than that of Sample A ($8\lambda_{A,GaInNAs}$=70nm). Since GaInNAs QW of Sample B has lower nitrogen content, the crystal defect density should be less than that of Sample A. This is evident in Fig.12 where the intensity and FWHM of GaInNAs QW of Sample B are higher and smaller, respectively. Hence the defect-assisted N-As diffusion effect at the Sample B GaInNAs/GaAs interface, which is reported as high during the beginning of PTA above 700 $^{o}$C [29], should be smaller that that of Sample A. By the same argument, the wavelength shift contributed by defect-assisted N-As diffusion effect in Sample B is smaller than that of Sample A. Since $8\lambda_{B,GaInNAs}$ (87nm) is larger than $8\lambda_{A,GaInNAs}$ (70nm), the residual-strain induced interdiffusion and the defect-induced diffusion are the dominant effect that contributed to the large PL wavelength shift of the GaInNAs QW of Sample B. Hence, it could be concluded that defect-assisted N-As diffusion is the dominant mechanism that results in the large wavelength shift in GaInNAs QWs with low In compositions. On the other hand, residual-strain induced interdiffusion and the defect-induced diffusion dominates when the In composition is high.
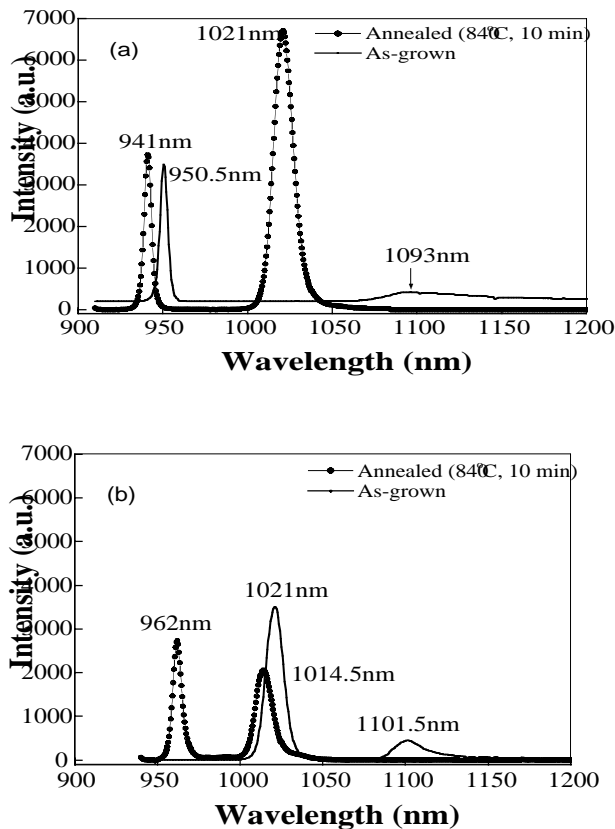
The X-ray diffraction (XRD) 004 scans of were used to investigate the structural change of Sample A and Sample B before PTA (as-grown) and after PTA (annealed). In Fig.13(a) and Fig.13(b), the humps on the negative-angle region increases in intensity and shifted towards the substrate peak after PTA at 840$^{o}$C. Larger shifting of the humps



Fig.12: The PL spectra from as-grown and annealed
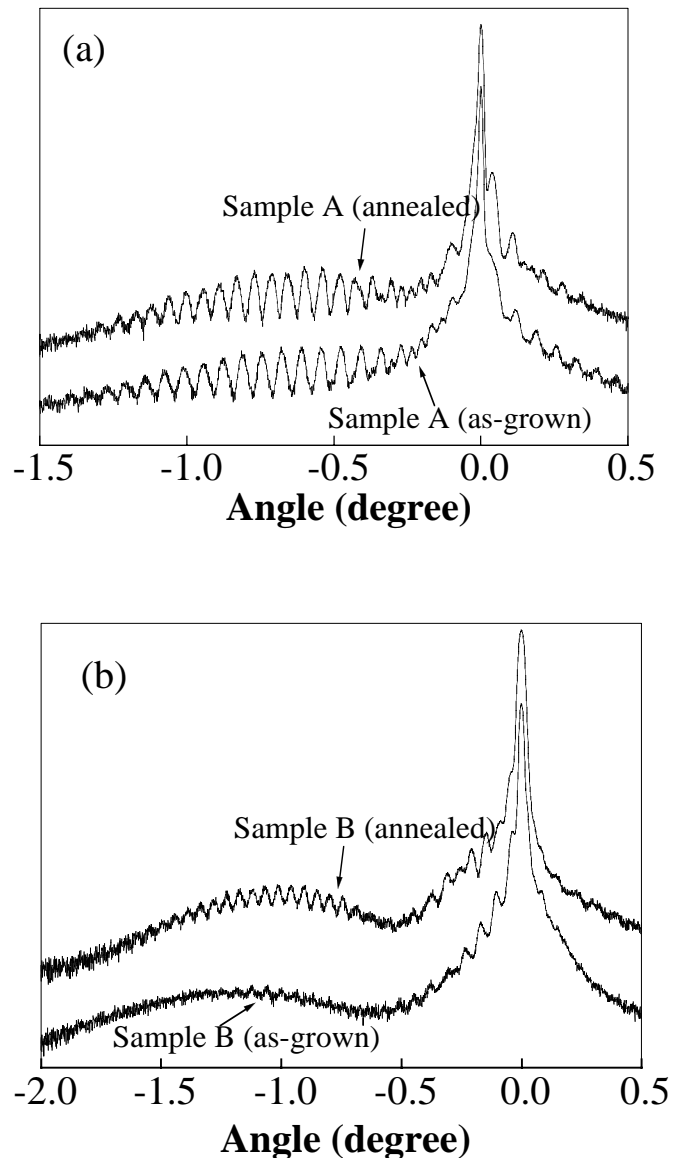MN073(a) and MN074(b) samples.



Fig.13: The XRD spectra from as-grown and annealed MN073 and MN074 samples.

positions is observed for Sample B compared to Sample A indicating much more reduction of In compositions in the highly strained Sample B. This further supports the argument of residual-strain induced wavelength shift in the above discussions. In addition, very clear and high peak-to-peak intensities of the Pandeloesung fringes on the humps were

observed after the PTA process for both the as-grown and annealed curves in Fig.13(a) (Sample A), indicating abrupt layer interface. The lower peak-to-peak intensities of the Pandeloesung fringes in Fig.13(b) shows that the layer interfaces are less well defined and form the source of defects at the interface. This is consistent with the observations in the PL FWHM studies in Fig.13 and further supports the defect-assisted interdiffusion effect that partly results in the large peak shift in GaInAs and GaInNAs QWs.

## IV. SUMMARY

In this article, we report an attempt of extending the InGaAsN materials towards 1.3μm and 1.55μm wavelength. All these InGaAsN samples are grown in a plasma-assisted solid-source molecular-beam epitaxy (SS-MBE) system. Our experiments revealed that the nitrides could be grown with both direct nitrogen beam and dispersive nitrogen. The nitrogen incorporation rate could be reduced by the presence of indium flux. The interaction between nitrogen and indium might lead to 3D growth mode and growth dynamics. It is proved that the increasing growth rate reduces the nitrogen incorporation efficiency. The data for nitrogen sticking coefficient are somewhat contradictive. The growth with dispersive nitrogen source causes the improvement of material quality. Fixed indium flux is a better way for the wavelength control. Also, we report some growth optimization work for better PL property and the annealing effect on the samples. Literature is sometimes reviewed for comparison.

## REFERENCES

[1] N.K.Dutta and R.J.Nelson, Appl.Phys.Lett.38, 407(1981).

[2] M.Kondow, K.Uomi, A.Niwa, T.Kitatani, S.Watahiki, and Y.Yazawa, Jpn.J.Appl.Phys., Part 1 35, 1273(1996).

[3] X.Yang, J.B.Heroux, M.J.Jurkovic, and W.I.Wang. Appl.Phys.Lett.76, 795(2000).

[4] Mark Telford, III-Vs Review, Vol.14, No.6, pp.28(2001).

[5] S.Sato and S.Satoh. IEEE Photonics Technol. Lett.11, 1560(1999).

[6] A.Wanger, C.Ellmers, F.Hohnsdorf, J.Koch, C.Agert, S.Leu, M.Holfmann, W.Stolz, and W.W.Ruhle, Appl.Phys.Lett. 76, 271(2000).

[7] M.Weyers and M.Sato. Appl.Phys.Lett.62, 1396(1993).

[8] M.Kondow, K.Uomi, T.Kitatani, S.Watahiki and Y.Yazawa. J.Cryst.Growth 164, 175(1996).

[9] Y.Qiu, S.A.Nikishin, H.Temkin, N.N.Faleev and Yu. A. Kudriavtsev. Appl.Phys.Lett. 70, 3242(1997).

[10] W.G.Bi and C.W.Tu. Appl.Phys.Lett.70, 1608(1997).

[11] S.Z.Wang, S.F.Yoon, W.K.Loke, T.K.Ng, and W.J.Fan, J.Cryst.Growth(submitted, 2001).

[12] S.Z.Wang, S.F.Yoon, W.K.Loke, T.K.Ng, and W.J.Fan, J.Vac.Sci.Technol.(submitted, 2001).

[13] J.C.Harmand, G.Ungaro, L.Largeau, and G.Le Roux. Appl.Phys.Lett.77, 2482(2000).

[14] E.Tournie, M.-A.Pinault, S.Vezian, J.Massies, and O.Tottereau, Appl.Phys.Lett.77, 2189(2000).

[15] H.P.Xin, K.L.Kavanagh, and C.W.Tu, J.Cryst.Growth 208, 145(2000).

[16] Z.Pan, L.H.Li, W.Zhang, Y.W.Lin, and R.H.Wu, Appl.Phys.Lett.77, 214(2000).

[17] P.R.Chalker, H.Davock, S.Thomas, T.B.Joyce, T.J.Bullough, R.J.Potter, N.Balkan, J.Cryst.Growth 233, 1(2000).

[18] T.Kitatani, K.Nakahara, M.Kondow, K.Uomi, T.Tanaka, J.Cryst.Growth 209, 345(2000).

[19] A.Yu.Egorov, D.Bernklau, B.Borchert, S.Illek, D.Livshits, A.Rucki, M.Schuster, A.Kaschner, A.Hoffmann, Gh.Dumitras, M.C.Amann, H.Riechert, J.Cryst.Growth 227,545(2001).

[20] S.G.Spruytte, M.C.Larson, W.Wampler, C.W.Coldren, H.E.Petersen, J.S.Harris, J.Cryst.Growth 227,506(2001)].

[21] T.Kitatani, M.Kondow, K.Nakahara, T.Tanaka, IEICE Trans.Electron.E83C(6), 830(2000).

[22] EPI Application Note, 97-3(1997).

[23] T.H.Myers, M.R.Millecchia, A.J.Ptak, K.S.Ziemer, and C.D.Stinespring. J.Vac.Sci.Technol.B17, 1654(1999).

[24] L.H.Li, Z.Pan, W.Zhang, Y.W.Lin, Z.Q.Zhou and R.H.Wu. J.Appl.Phys.87,245(2000).

[25] L.H.Li, Z.Pan, W.Zhang, Y.W.Lin, X.Y.Wang, and R.H.Wu. J.Cryst.Growth 227-228, 527(2001).

[26] T.K.Ng, S.F.Yoon, S.Z.Wang, W.K.Loke, W.J.Fan, submitted to J.Vac.Sci.Technol.(2001).

[27] R.A.Mair, J.Y.Lin, H.X.Jiang, E.D.Jones, A.A.Allerman, S.R.Kurtz, Appl.Phys.Lett.76, 188(2000).

[28] I.A.Buyanova, W.M.Chen, and B.Monemar, MRS Internet J.Nitride Semicond.Res.6, 2(2001).

[29] Z.Pan, L.H.Li, W.Zhang, Y.W.Lin, R.H.Wu, W.Ge, Appl.Phys.Lett.77, 1280(2000).

[30] Z.Pan, T.Miyamoto, S.Sato, F.Koyama, K.Iga, Jpn.J.Appl.Phys., Part 1 38, 1012(1999).

[31] S.W.Ryu, I.Kim, B.D.Choe, W.G.Jeong, Appl.Phys.Lett.67, 1417(1995).